

The strength of acrylic bone cements and acrylic cement-stainless steel interfaces

Part 2 *The shear strength of an acrylic cement-stainless steel interface*

P. W. R. BEAUMONT

Department of Engineering, University of Cambridge, Cambridge, UK

B. PLUMPTON

New Hall, Cambridge, UK

The mechanical behaviour of a joint made from two dissimilar materials is determined in part by the transfer of stress across the interface between the components. A technique involving a shear lag analysis and pull-out experiments on stainless steel rods which have been embedded in a surgical acrylic bone "cement" has been used to evaluate the shear strength and shear modulus of a stainless steel-acrylic bone "cement" interface. The interfacial shear strength is then compared with a theoretical estimation of the shear stresses acting upon a femoral hip prosthesis-acrylic bone "cement" interface. Trapped blood between the stainless steel and acrylic bone "cement" was found to decrease the shear strength and shear modulus of the interface significantly.

1. Introduction

The interfacial bond between a femoral stem of a hip prosthesis and an acrylic bone *cement* can influence various aspects of the mechanical and fracture behaviour of a total hip joint replacement; it can effect the transfer of load between the prosthesis and bone, the shear strength and shear modulus of the interface, and the mode of failure of the hip replacement. This paper describes a method for measuring the shear stress at a stainless steel-acrylic bone *cement* interface, and a study of the effects of blood serum upon the shear strength and shear modulus of the interface. The approach is straightforward; it involves, on the one hand, the use of a shear lag analysis, and on the other, an evaluation of experimental data from pull-out tests on stainless steel rods embedded in an acrylic bone *cement* matrix.

2. Materials and specimen design

A surgical bone *cement* known as SIMPLEX P, consisting of PMMA powder and liquid methyl methacrylate monomer, was prepared as described in Part 1. The *cement*, whilst in the "doughy

state", was firmly packed, using the fingers, around a stainless steel rod centrally positioned inside a mild steel, cylindrical-shaped mould (Fig. 1). Careful positioning of the rod ensured that the

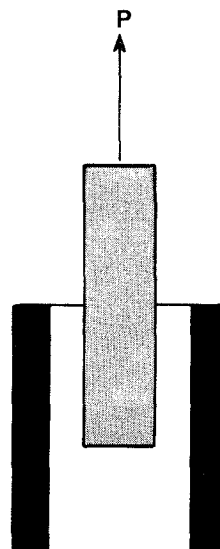


Figure 1 A schematic representation of the rod pull-out experiment.

embedded length could be varied between 2 mm and 35 mm approximately. Polymerization of the acrylic bone *cement* was essentially complete within about 20 min of specimen preparation; pull-out tests on the stainless steel rods took place 24 h later. In a few cases, the stainless steel rod was dipped first into a blood serum before packing acrylic bone *cement* around it.

3. Experimental details and analysis

3.1. Pull-out test

The specimens were loaded uniaxially in an Instron mechanical testing machine. A tensile force was applied to the rod by connecting the protruding end of the rod to the load cell and the mould to the cross-head of the machine. For all tests, a constant cross-head speed of 2 mm min⁻¹ was used. The test was continued until the rod had been completely pulled out of its socket. In this test, a maximum interfacial shear stress occurs at the point where the rod enters the matrix; if the shear strength of the interface τ_i is exceeded, then debonding will result, and the debonded zone will extend along the embedded length of rod. Whether the growth of the debonded zone becomes unstable or whether it grows in a controlled manner will depend upon the frictional forces acting between the separated surfaces and upon the value of τ_i . The initial "frictional" shear stress is given by

$$\tau' = \frac{P'}{2\pi r l_e} \quad (1)$$

where P' is the maximum post-failure load to start the rod sliding, r is the radius of the rod and l_e is the embedded length of rod in the matrix.

For any tensile load P on the rod, the average interfacial shear stress is given by

$$\tau_{av} = \frac{P}{2\pi r l_e} \quad (2)$$

3.2. Shear lag model

The shear strength and shear modulus of the stainless steel-acrylic bone *cement* interface can be estimated using a shear lag analysis and the experimental data obtained from the pull-out tests. At any point x on the surface of an embedded fibre or rod, the shear stress τ is given by [1]

$$\tau(x) = \frac{P\alpha}{2\pi r} (\sinh \alpha x - \coth \alpha l_e \cosh \alpha x) \quad (3)$$

where α is a constant for the system given by

$$\alpha = \left(\frac{2G_i}{b_i r E_f} \right)^{1/2} \quad (4)$$

G_i is the shear modulus of the interface having an effective thickness of b_i . E_f is the Young's modulus of fibre or rod.

Combining Equations 2 and 3;

$$\frac{\tau(x)}{\tau_{av}} = \alpha l_e (\sinh \alpha x - \coth \alpha l_e \cosh \alpha x) \quad (5)$$

Since the interfacial shear stress reaches a maximum value at the point $x = 0$,

$$\frac{\tau_{max}}{\tau_{av}} = \alpha l_e \coth \alpha l_e \quad (6)$$

As the embedded length of rod tends towards zero ($l_e \rightarrow 0$), then τ_{max}/τ_{av} tends towards unity, i.e. τ_{max} tends towards τ_{av} .

The maximum interfacial shear stress τ_{max} , can be estimated using the experimental data plotted in the form of τ_{av} as a function of l_e , and extending the curve so as to cut the τ_{av} axis at $x = 0$. Next, the shear modulus of the interface can be estimated using Equation 6. For any embedded length of rod, τ_{av}/τ_{max} can be determined; a corresponding value of αl_e can be obtained from Equation 6. The shear modulus can then be calculated using the expression for α and the appropriate values of E_f , r and b_i .

4. Results and discussion

4.1. Load/displacement curve

Typical load/displacement curves are shown in Figs. 2 and 3 for a stainless steel rod being pulled

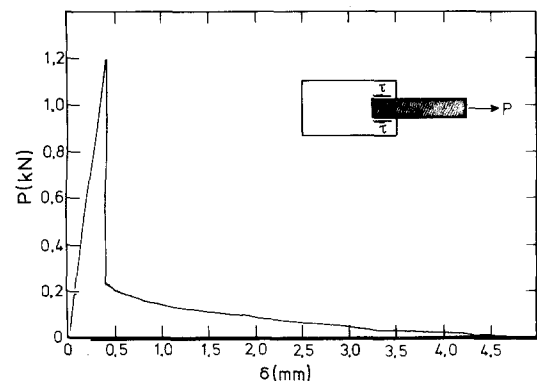


Figure 2 A typical load/displacement diagram for pulling out a stainless steel rod embedded to a depth of 5 mm.

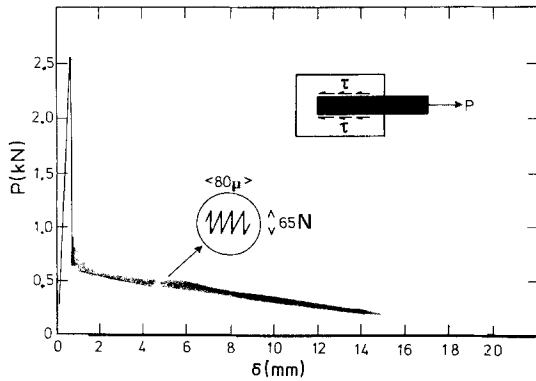


Figure 3 A typical load/displacement diagram for pulling out a stainless steel rod embedded to a depth of 20.5 mm. (The insert is a magnification of the saw-tooth pattern associated with the “stick–slip” mode of failure.)

out of the acrylic bone *cement* matrix. The principle features of the curves include: (1) an initial linear portion increasing up to a maximum load P_{\max} ; (2) a precipitous drop in load when P reaches P_{\max} to a new load P' where $P' = 0.3P_{\max}$ approximately; and (3) a post-failure saw tooth pattern in the load/displacement curve.

The distance d_n moved by the rod per “stick–slip” cycle, and the difference ΔP_n between maximum and minimum loads in that cycle, remain essentially constant as the rod is slowly extracted from its socket; eventually, the load falls to zero (Fig. 3). For small values of embedded length ($l_e < 10$ mm) the “stick–slip” failure mechanism is absent; at values of l_e between 10 mm and 20 mm, it is observed a few times at the beginning of rod pull-out only. Fig. 4 shows the average distance moved by the rod per “slip–stick” cycle as a function of l_e ; a plateau exists at $d_n = 25 \mu\text{m}$ approx-

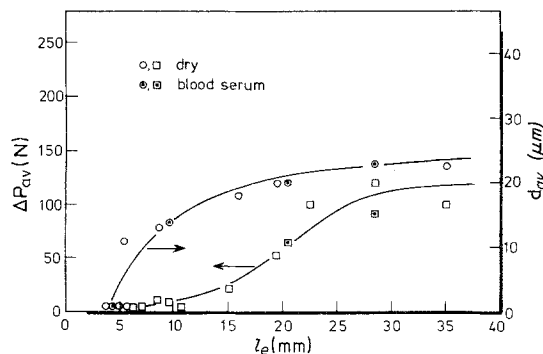


Figure 4 Variation of the average “stick–slip” force interval ($P_{n(\max)} - P_{n(\min)}$) and the average distance moved (d_{av}) by the stainless steel rod in a “stick–slip” cycle as a function of embedded length.

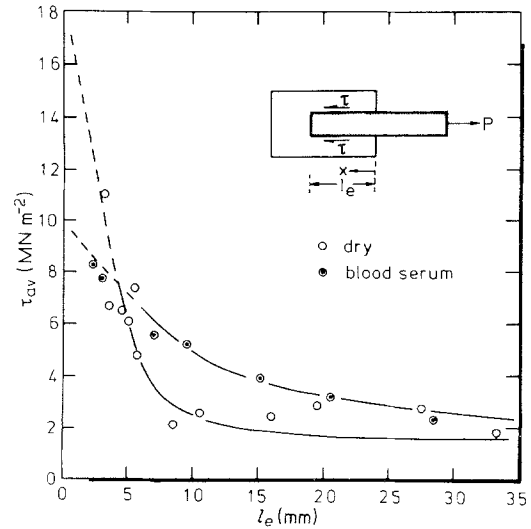


Figure 5 Average shear stress (τ_{av}) acting at a stainless steel–acrylic bone *cement* interface as a function of embedded length of rod. (Data collected for dry (clean) interfaces and interfaces containing trapped blood serum.)

imately. It is interesting to note that the average distance between surface irregularities, (“peaks” and “valleys”), measured on the surface of the stainless steel rod using a Talysurf is of the order of $25 \mu\text{m}$ also.

4.2. Interfacial shear stress

The variation of τ_{av} with embedded length of stainless steel rod is shown in Fig. 5. For values of $l_e > 25$ mm, τ_{av} is about $2.1 (\pm 0.5) \text{ MN m}^{-2}$. An extrapolation of the curve to $l_e = 0$, is difficult to make precisely but τ_{\max} has been estimated to be $18 (\pm 2) \text{ MN m}^{-2}$. The initial “frictional” shear stress, τ' , has a mean value of $1.6 (\pm 0.5) \text{ MN m}^{-2}$, and is independent of l_e .

Some preliminary experiments were carried out to determine the effects of load cycling upon the residual shear strength of the metal–polymer interface. Even after 5000 cycles at $0.6P_{\max}$, there was no noticeable effect upon the shape of the quasi-static load/displacement curve or upon τ_{av} .

The presence of a blood serum trapped between the surfaces of the stainless steel and acrylic bone “cement” had no effect whatsoever on the shape of the load/displacement curve; however, the experimental points of τ_{av} lie on a much smoother curve (Fig. 5) compared to the data obtained using the clean stainless steel rods. The maximum shear stress at the interface containing the blood serum

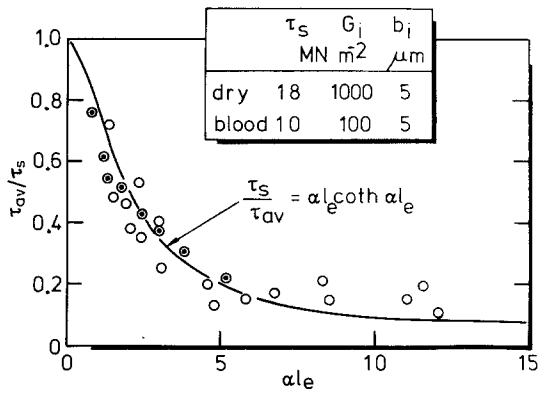


Figure 6 Ratio of τ_{av}/τ_s as a function of αl_e (Equation 6).

τ_{\max} was estimated to be $10.0 (\pm 1) \text{ MN m}^{-2}$; the initial "frictional" shear stress τ' was equal to $0.9 (\pm 0.2) \text{ MN m}^{-2}$, approximately an order of magnitude less than the maximum interfacial shear stress, and nearly a factor 2 less than for the uncontaminated interface.

4.3. Shear lag analysis

Fig. 6. shows a plot of τ_{av}/τ_{\max} as a function of αl_e (Equation 6), together with experimental data. If the shear modulus of the interface G_i is assumed to be equal to the shear modulus of the matrix G_m , ($G_m = 1 \text{ GN m}^{-2}$ approximately), then the experimental points lie upon the theoretical curve very well for a value of b_i equal to $5 \mu\text{m}$ and a shear strength τ_s equal to 18 MN m^{-2} for the uncontaminated interface. The value of b_i is approximately equal to the centre line average value of $3 \mu\text{m}$ for the surface irregularities of the stainless steel rod, measured using a Talysurf. Since b_i is a constant for all specimens, then the results obtained for samples containing blood serum at the interface indicate an interfacial shear modulus G_i of 100 MN m^{-2} and a shear strength τ_s of 10 MN m^{-2} . This represents a fall in the values of G_i and τ_s by approximately a factor of 10 and 2, respectively, compared to the values for the uncontaminated interface. For comparison purposes, the shear strength of the acrylic bone cement has been estimated as 45 MN m^{-2} [2].

It is important to note that McNeice [3] using a finite element analysis has estimated the maxi-

imum shear stress at a femoral stem-acrylic bone cement interface to be $16 (\pm 2) \text{ MN m}^{-2}$. The value is extremely close to the measured shear strength of the uncontaminated interface and suggests that in practice, the shear strength may be exceeded very early in the life-time of the hip prosthesis. This seems extremely likely of interfaces containing trapped blood.

5. Conclusions and implications

A test technique based upon pull-out tests and shear lag theory appears to offer a method for evaluation of the shear strength and shear modulus of a metal-polymer interface. For a stainless steel-acrylic bone cement system, the interfacial shear strength was of the order of 18 MN m^{-2} ; this is about one-third of the shear strength of acrylic bone cement. This value is very close to a theoretical estimation of the shear stresses that act at a femoral prosthesis-acrylic bone cement interface determined by McNiece using a finite element analysis. It seems likely, therefore, that working shear stresses at a hip prosthesis-acrylic bone cement interface, can exceed the shear strength of the bond and cause debonding. The presence of trapped blood reduces the shear strength and increases the likelihood of premature bond failure. Increasing the surface roughness of the stainless steel prosthesis may effectively increase the shear strength and shear modulus of the interface, but the existence of surface irregularities will inevitably reduce the fatigue life of the prosthesis.

Acknowledgement

We would like to thank Mr L. Shadbolt of Homedica Inc. for supplying us with samples of SIMPLEX P surgical acrylic bone cement.

References

1. L. B. GRESZCZUK, ASTM STP 452 (1969) 42.
2. P. W. R. BEAUMONT and R. J. YOUNG, "Plastics in Medicine and Surgery", (Plastic and Rubber Institute, London, 1975) 7.1.
3. G. M. McNIECE and H. C. AMSTUTZ, Proceedings of the 5th International Congress on Biomechanics, University of Jyraskyla (1975).

Received 25 November 1976 and accepted 21 January 1977.